
A MATHEMATICAL MODEL FOR ARCH FINGERPRINT

A PREPRINT

Ibrahim Jawarneh

Department of Mathematics
Al-Hussein Bin Talal University
Ma'an, P.O. Box (20), 71111, Jordan
ibrahim.a.jawarneh@ahu.edu.jo

Nesreen Alsharman

Computer Science
The World Islamic Sciences and Education University
Amman, Jordan
nesreen.alsharman@wise.edu.jo

October 5, 2020

ABSTRACT

In this paper, different categories of the arch fingerprint are modelled in a general dynamical system using ordinary differential equations with a parameter $\theta > 0$. We study its global dynamics and analyze the existence and stability of equilibria. Numerical simulations using Maple show the matching between real images of categories of arch fingerprint and phase portraits of the considered dynamical system.

Keywords Arch fingerprint · Plain arch fingerprint · Tented arch fingerprint · Strong arch fingerprint · Numerical simulations of categories of arch fingerprint.

1 Introduction

Fingerprints are patterns, made by friction ridges of a human finger, which appear on the pads of the fingers and thumbs. The fingerprints is the most accurate and reliable for identifying person, since fingerprints are most unique biometric characteristics to any person; therefore it is used in forensic divisions worldwide for security, and in criminal cases where even the twins have non-identical fingerprints. Early study about fingerprints appeared in 1892 by Sir Francis Galton in his book, *finger prints* [4]. The patterns of fingerprints are classified into three general types; loop, whorl, and arch, many studies indicate that arch patterns are observed in about 5% of all fingerprints, see [1, 4, 5].

The arch patterns display a relatively horizontal ridges run from the left to the right side of the fingerprint with growth in the center. This paper discusses three categories of arch fingerprint which are shown in figure 1 and we depend on it as a database of the classes of arch fingerprint.

- Plain arch in which the ridges flow relatively horizontally with a little rise in the middle where delta is not clear here, see picture (a) in figure 1.
- Tented arch is similar to the plain arch with a bigger rise, and at least one ridge with short length is vertically oriented in the middle where delta is clear here, see picture (b) in figure 1.
- Strong arch is similar to the tented arch with many relatively longer ridges are vertically oriented in the middle where delta is very clear here, this category looks like Christmas tree, see picture (c) in figure 1.

A few studies talked about modelling of arch fingerprint, Huckemann et al. [6] proposed a model based on quadratic differentials that describes arch fingerprint but they do not show the results for a tented arch since they considered it as a special case of a loop. Moreover, they did not study the strong arch. The conditional cosine functions were used for modeling arch-typed fingerprints in the full plane without going over specific classes, see [2, 7, 9]. We did not find any study proposed a general mathematical model for all classes of arch fingerprint as we focus in this paper. Fingerprints can be captured as graphical ridge and valley patterns, so we start to put a model which simulates the ridge flow and pattern types in the above classes. Using differential equations in creating dynamical system that describes plain, tented, and strong arch fingerprint require understanding the behaviour of the ridges in these classes and how much the delta is clear in each class. In this case the flow of the phase portrait of this system represents the ridges in the fingerprint, so

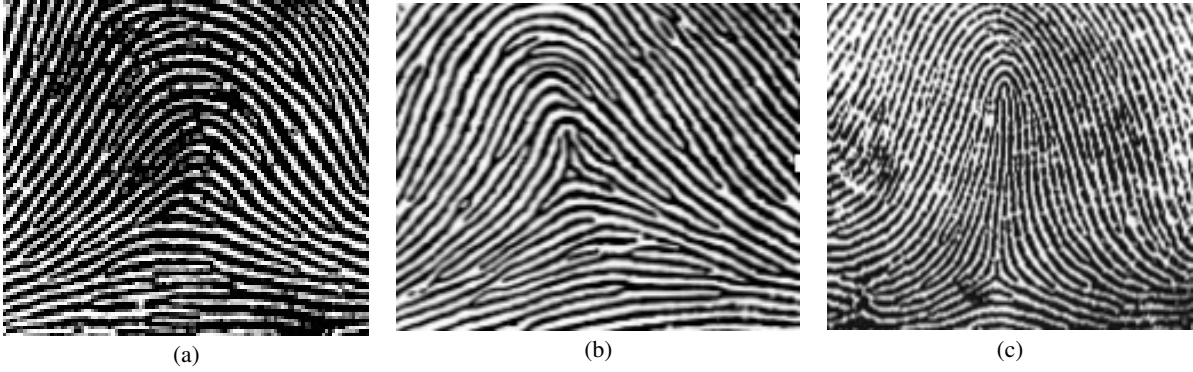


Figure 1: (a) Plain arch fingerprint, (b) tented arch fingerprint and (c) strong arch fingerprint

we think about the deformation of the phase portrait of straight flow to generate such system. We proceeded by trial and error to approximate the following dynamical system that represents the general map of the above categories of the arch.

$$\begin{aligned} \dot{x} &= y^2, \\ \dot{y} &= -\theta x, \quad \theta > 0. \end{aligned} \quad (1)$$

This paper is organized as follows : In the next section, we study the stability of the equilibria of system (1). In section 3 we go over different values of θ in the dynamical system (1) to simulate the categories of the arch fingerprint. In section 4 we conclude the results of the proposed model.

2 Steady States and Their Stability

To study the stability of the system (1), we find the equilibria first, which are the solutions of the following equations:

$$0 = y^2, \quad (2)$$

$$0 = -\theta x, \quad (3)$$

and are given by $E_0 = (0, 0)$ which is called equilibrium point or singular point. The Jacobian matrix of (1) takes the form

$$J = \begin{bmatrix} 0 & 2y \\ -\theta & 0 \end{bmatrix}. \quad (4)$$

The Jacobian matrix evaluated at the equilibrium point $E_0 = (0, 0)$ is

$$J(E_0) = \begin{bmatrix} 0 & 0 \\ -\theta & 0 \end{bmatrix}. \quad (5)$$

From the Jacobian matrix (5), the eigenvalues of $J(E_0)$ are $\lambda_{1,2} = 0$ which means degenerate nonhyperbolic equilibrium point, the phase portrait for this system is shown in section 3. In all categories of arch fingerprints, we see that a deleted neighborhood of the origin consists of upper and lower hyperbolic sectors, also it consists of left and right separatrices. This type of critical point is called a cusp, see [8]. The cusp plays the role of the delta in the above description of the categories of arch fingerprint. But the flow which is located above the origin makes different types of the angle depending on the value of θ , for example we have obtuse angle in plain category, around right angle in tented category, and acute angle in strong category.

3 Simulations and Numerical Results

In this section, we study the system (1) with different values of θ and display its simulations and their matching images of the above categories of the arch fingerprint. We use bold red lines to represent the separatrices, the green lines at different initial conditions above x -axis to show the above hyperbolic sector, and the brown line at different initial conditions below x -axis to display the below hyperbolic sector.

3.1 Plain arch fingerprint

When θ is very small and closed to zero in (1), the flow of phase portrait is relatively horizontally with a slight growth in the middle as in figure 2. For example consider system (1) with $\theta = 0.001$.

Example 3.1.

$$\begin{aligned} \dot{x} &= y^2, \\ \dot{y} &= -0.001x. \end{aligned} \tag{6}$$

Figure 2 shows the simulation of the example (3.1) using Maple. Figure 3 explains a closer look at the neighborhood of

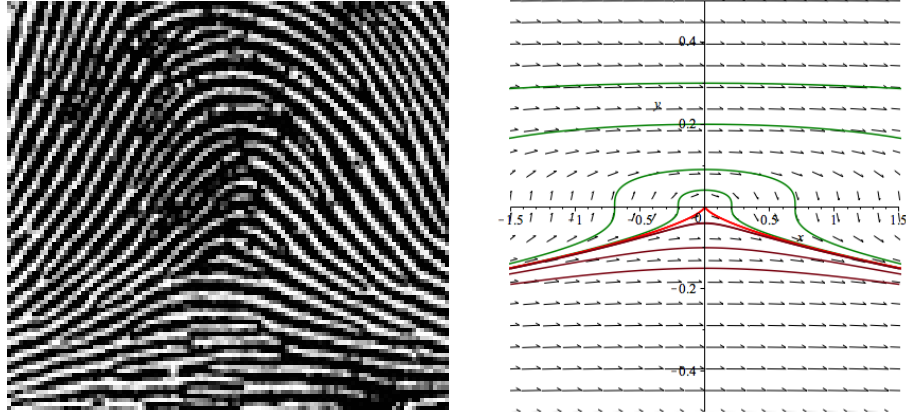


Figure 2: Simulation of the plain fingerprint

the origin, we have explained the separatrices in the phase portrait, and we use a thin blue line to determine the region of hyperbolic sectors, and hence the origin is cusp fixed point which represents the delta in the plain arch fingerprint image. We notice the similarity between the flow in the phase portrait of the system (6) and the layout of the ridges in the image of the plain arch fingerprint.

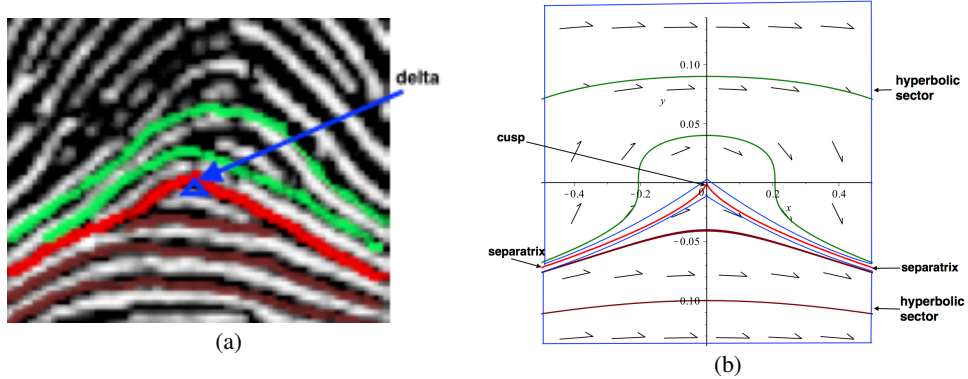


Figure 3: (a) Neighborhood of the delta in the image of the plain arch fingerprint and (b) Neighborhood of the origin in the phase portrait of example 3.1 .

3.2 Tented arch fingerprint

If we increase θ reaching around 0.5 in (1), the flow rises more in the middle with a smaller angle above the origin than the case of plain type. In this case we get phase portrait looks like tented arch, for example consider system (1) with $\theta = 0.5$.

Example 3.2.

$$\begin{aligned} \frac{dx}{dt} &= y^2, \\ \frac{dy}{dt} &= -0.5x. \end{aligned} \tag{7}$$

The phase portrait of the example (3.2) is shown in figure 4, and figure 5 illustrates a focused attention around the origin in the phase portrait and the delta in the tented arch fingerprint image. It is clear that the smooth flow and the arrangement of the ridges are similar.

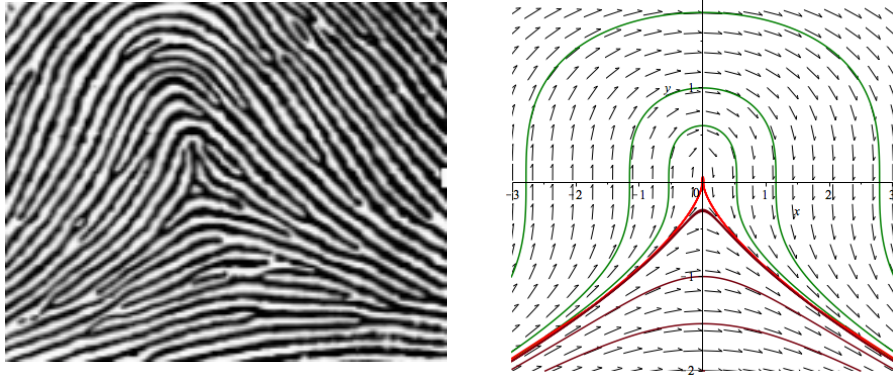


Figure 4: Simulation of the tented arch fingerprint

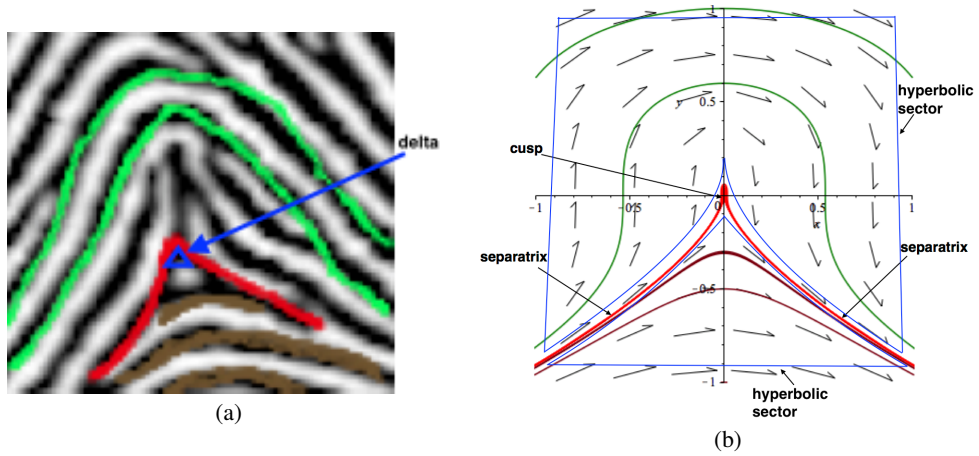


Figure 5: (a) Neighborhood of the delta in the image of the tented arch fingerprint and (b) Neighborhood of the origin in the phase portrait of example 3.2 .

3.3 Strong arch fingerprint

If θ grows up enough around the value $\theta = 5$, the flow stretched longer vertically in the middle with a cusp at the origin making acute angle. This flow agrees with the general shape of the strong arch, for example consider system (1) with $\theta = 5$ we get the system (8).

Example 3.3.

$$\begin{aligned} \frac{dx}{dt} &= y^2, \\ \frac{dy}{dt} &= -5x. \end{aligned} \tag{8}$$

In figure 6 we see the matching between the image of strong arch and the phase portrait of example (3.3), and in figure 7 we see how the flow is narrowed about the origin point in a sharp vertical way to be identical with the ridges around the delta in the strong arch fingerprint image.

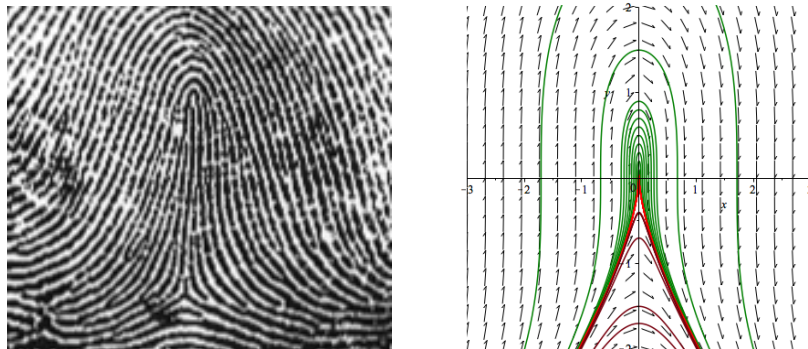


Figure 6: Simulation of the strong arch fingerprint

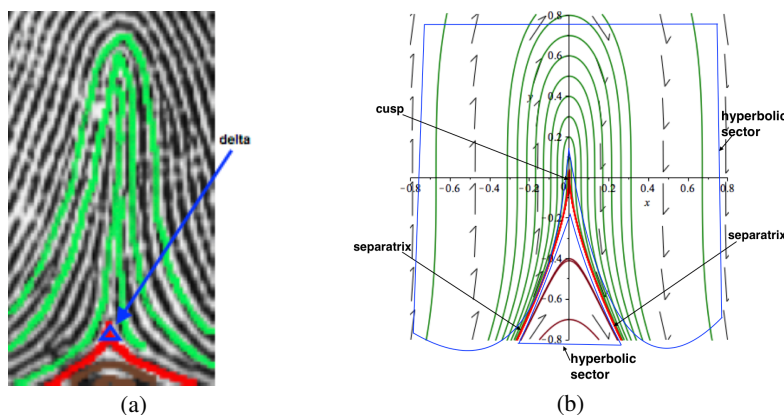


Figure 7: (a) Neighborhood of the delta in the image of the strong arch fingerprint and (b) Neighborhood of the origin in the phase portrait of example 3.3 .

4 Conclusion

The general shape of the flow of the considered dynamical system and the shape of the ridges in the images of the categories of the arch fingerprint are almost identical to each other.

References

- [1] de Jongh A, Lubach AR, Lie Kwie SL, Alberink. Measuring the Rarity of Fingerprint Patterns in the Dutch Population Using an Extended Classification Set. *Journal of Forensic Sciences* 2019.
- [2] Cappelli, R., Lumini, A., Maio, D. and Maltoni, D. Fingerprint Image Reconstruction from Standard Templates. *IEEE Trans. Pattern Analysis and Machine Intelligence*, 29(9), pages 1489–1503, 2007.
- [3] Ford, R. Image models for flow field analysis, representation, and compression: A dynamical systems approach, Ph.D.thesis. *University of Arizona* 1994.
- [4] Galton, F. Fingerprint prints. *MacMillan and co., London* 1892.
- [5] Henry, E. R. Classification and uses of fingerprint prints. *London: George Rutledge & Sons Ltd.* 1900.
- [6] Huckemann, S., Hotz, T. and Munk, A. Global Models for the Orientation Field of Fingerprints: An Approach Based on Quadratic Differentials. *IEEE Transactions on Pattern Analysis and Machine Intelligence*, 30(9), pages 1507–1519, 2008.
- [7] Maltoni, D., Maio, D., Jain, A.K and Prabhakar S. Handbook of Fingerprint Recognition. *Springer-Verlag, New York* 2009.
- [8] Perko, Lawrence. Differential equations and dynamical systems. *Springer-Verlag, New York* 2001.
- [9] Wang, Yi and Hu, Jiankun. Global Ridge Orientation Modeling for Partial Fingerprint Identification. *IEEE Transactions on Pattern Analysis and Machine Intelligence*, 33(1), pages 72–87, 2011.